Spectroscopy of Stripe Order in $La_{1.8}Sr_{0.2}NiO_4$ Using Resonant Soft X-Ray Diffraction

C. Schüßler-Langeheine,[1] J. Schlappa,[1] A. Tanaka,[2] Z. Hu,[1] C. F. Chang,[1] E. Schierle,[3] M. Benomar,[1] H. Ott,[1,3] E. Weschke,[3] G. Kaindl,[3] O. Friedt,[1,4] G. A. Sawatzky,[5] H.-J. Lin,[6] C. T. Chen,[6] M. Braden,[1] and L. H. Tjeng[1]

[1]*II. Physikalisches Institut, Universität zu Köln, Zülpicher Strasse 77, D-50937 Köln, Germany*
[2]*Department of Quantum Matter, ADSM, Hiroshima University, Higashi-Hiroshima 739-8530, Japan*
[3]*Institut für Experimentalphysik, Freie Universität Berlin, Arnimallee 14, D-14195 Berlin, Germany*
[4]*Laboratoire Léon Brillouin, CEA-Saclay, 91191 Gif-sur-Yvette Cedex, France*
[5]*Department of Physics and Astronomy, University of British Columbia, 6224 Agricultural Road, Vancouver, British Columbia, Canada V6T 1Z1*
[6]*National Synchrotron Radiation Research Center, Hsinchu 30076, Taiwan*

(Received 15 February 2005; published 6 October 2005)

Strong resonant enhancements of the charge-order and spin-order superstructure-diffraction intensities in $La_{1.8}Sr_{0.2}NiO_4$ are observed when x-ray energies in the vicinity of the Ni $L_{2,3}$ absorption edges are used. The pronounced photon-energy and polarization dependences of these diffraction intensities allow for a critical determination of the local symmetry of the ordered spin and charge carriers. We found that not only the antiferromagnetic order but also the charge-order superstructure resides within the NiO_2 layers; the holes are mainly located on in-plane oxygens surrounding a Ni^{2+} site with the spins coupled antiparallel in close analogy to Zhang-Rice singlets in the cuprates.

DOI: 10.1103/PhysRevLett.95.156402 PACS numbers: 71.45.Lr, 61.10.Dp, 71.27.+a, 75.50.Ee

Doped charge carriers in strongly correlated oxides are often found to induce ordered periodic arrangements at low temperatures. The first system where such a phenomenon was observed by scattering techniques is hole-doped La_2NiO_4: Electron and neutron diffraction experiments found in $La_{2-x}Sr_xNiO_{4+\delta}$ stripelike superstructures [1–3], which were interpreted in terms of charge ordering. The hole-rich stripes form antiphase domain walls for the antiferromagnetic order on the Ni^{2+} sites, and the spacing between them was determined to be inversely proportional to the hole concentration $n_h = x + 2\delta$. Similar claims have been made for the isostructural high-T_c superconductors $La_{2-x}Sr_xCuO_4$ [4], although recently competing models have been proposed [5,6].

Understanding the physics behind the formation of the superstructures in $La_{2-x}Sr_{0.2}NiO_4$ is still a difficult issue [7], which is mainly because the electronic structure related to these stripe phases is not known. The standard neutron and x-ray scattering techniques used so far are not directly sensitive to charge: they pick up mainly the lattice modulations that are induced by doping. It is therefore not clear whether one should really model the stripe phases as an ordering of Ni^{2+} and Ni^{3+} ions. Spectroscopic techniques, for instance, have revealed that doping introduces substantial amounts of holes in the oxygen band [8,9], thereby raising the question whether a description in terms of oxygen hole ordering would be more appropriate. To make things more confusing, there is not even an agreement to what extent and with which symmetry the oxygen holes are bound to the Ni [9–11].

In this Letter we present results from a new type of spectroscopic technique, namely, resonant diffraction using soft x rays. Here the diffraction involves virtual electronic excitations into unoccupied intermediate states [12], which lead to a characteristic modulation of the scattering cross section with photon energy. In particular, excitations in the vicinity of the transition metal $L_{2,3}$ ($2p \rightarrow 3d$) and rare-earth $M_{4,5}$ ($3d \rightarrow 4f$) absorption edges are known to be very sensitive to details of the electronic state of the ions [13–15]. Resonant diffraction is, in fact, a combination of spectroscopy and structure determination, and is therefore the most suitable and natural technique to study the electronic structure of superstructures in transition metal and rare-earth systems [16–23].

We carried out resonant diffraction experiments on $La_{1.8}Sr_{0.2}NiO_4$ at the Ni $L_{2,3}$ threshold for both the spin-order and charge-order superstructures. We observed pronounced photon-energy and polarization dependences of these diffraction intensities, which allow us to critically determine the local symmetry of the ordered spin and charge carriers. Using a quantitative microscopic theoretical model, we find that the holes are mainly located on the in-plane oxygens surrounding a Ni^{2+} site with the spins coupled antiparallel, in close analogy to Zhang-Rice singlets in the cuprates [24,25].

A single crystal of $La_{1.8}Sr_{0.2}NiO_4$ was grown by a traveling solvent method and characterized by neutron diffraction at the Orphée reactor, diffractometer 3T.1. In the following we use the orthorhombic notation with $b \approx a = 5.38$ Å and $c = 12.55$ Å. The diffraction features with the smallest momentum transfer are the charge-order peak at $(2\epsilon, 0, 1)$ and the spin-order peak at $(1 - \epsilon, 0, 0)$. For the doping level of our sample, ϵ is 0.278, and both peaks can be reached at the Ni $L_{2,3}$ and La $M_{4,5}$ resonances.

The soft x-ray scattering experiments were performed at the BESSY beam lines U49/2-PGM1 and UE52-SGM1, using the two-circle UHV diffractometer designed at the Freie Universität Berlin [26] in horizontal scattering ge-

ometry. The incoming light was linearly polarized either parallel to the scattering plane (π polarization) or perpendicular (σ polarization). A silicon-diode photon detector without polarization analysis was used with the angular acceptance set to 1° in the scattering plane and 5° perpendicular to it. The sample was cut and polished with a (101) surface orientation and mounted with the [100] and [001] directions in the diffraction plane. At 1010 eV photon energy the (002) structure Bragg peak could be reached and was used together with the superstructure peaks to orient the sample. Reference soft-x-ray absorption measurements on $La_{1.8}Sr_{0.2}NiO_4$ and $LaTiO_3$ have been performed at the Dragon beam line of the NSRRC in Taiwan.

The insets in Fig. 1 show scans through both superstructure peaks along the [100] (H) and [001] (L) directions, taken with π-polarized light and the photon energy tuned into the maximum of the Ni L_3 resonance. From the peak widths we determine the correlation length in the ab plane for charge order to about 200 Å and for spin order to about 300 Å. The order along the c direction is less developed with correlation lengths of 50 Å (40 Å) for spin (charge) order.

Figures 1(a) and 1(b) depict the photon-energy dependence of the superstructure intensities across the La $M_{4,5}$ and Ni $L_{2,3}$ edges for two different light polarizations plotted on the same vertical scale [27]. For both superstructure peaks the intensity shows a resonant enhancement mainly for photon energies about 851.6 eV, i.e., in the vicinity of the Ni L_3 white line. This is in striking contrast to the shape of the x-ray-absorption spectroscopy (XAS) data shown in Fig. 1(c), which are dominated by the La M_5 resonance at 833 eV and M_4 resonance at 849.2 eV. The gain in contrast for the Ni signal in the diffraction experiment comes from its sensitivity to only the ordered part of the system. The strong enhancement at the Ni resonance for both superstructure signals hence shows directly that not only the antiferromagnetic order but also the charge-order superstructure originates mainly from the NiO_2 layers. Both resonances show a dramatic polarization dependence. For the spin-order peak, the signal for σ polarization is only about 10% of that for π polarization; for the charge-order peak, the maxima at the L_3 and L_2 resonance when observed with σ-polarized light are shifted by about 1 eV towards higher photon energies as compared to the data taken with π-polarized light.

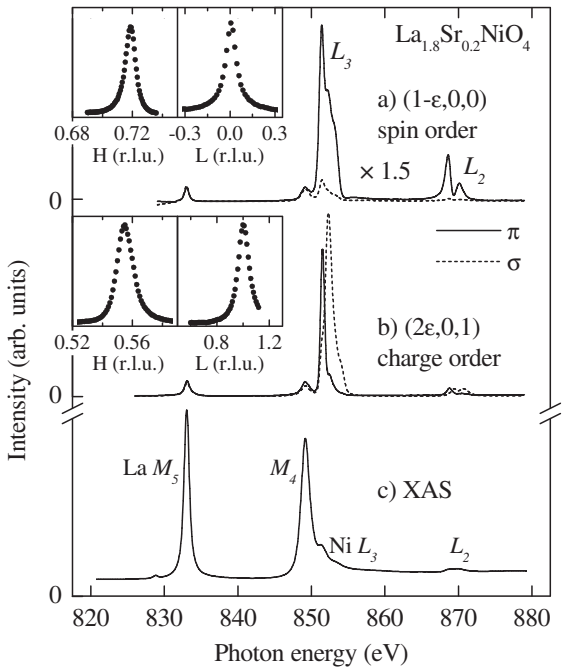

FIG. 1. Intensities of the (a) $(1-\epsilon, 0, 0)$ spin-order and (b) $(2\epsilon, 0, 1)$ charge-order superstructure peaks as a function of photon energy at 60 K for π-polarized (solid line) and σ-polarized (dashed line) light. The insets show scans through the respective superstructure peaks on a linear scale recorded with π-polarized light along the [100] (H) and [001] (L) directions; (c) x-ray absorption signal.

On a closer look, both superstructure peaks show a resonant enhancement at the La $M_{4,5}$ resonances as well. This is, however, a weak effect considering the relative intensities of the Ni and La resonances in the XAS signal. The fact that there is any enhancement of the charge- and spin-order signal at the La resonance indicates a coupling between Ni and La sites, which could be caused by the different bond lengths or by weak hybridization. A possible strong static dopant order in the La/Sr subsystem can be ruled out, since the superstructure peaks decrease above 65 K at both the Ni and the La resonances, while the shape of the resonances does not change in the temperature range between 35 and 120 K.

The contrast mechanism responsible for the spin-order peak is the different scattering cross section for different relative orientations of the electron spins and the polarization directions of the incoming and outgoing photons. From the weakness of the signal observed with σ-polarized light, which means that the electric-field vector of the incoming photons is parallel to the stripes, one can conclude that the Ni spins are essentially (but not perfectly) collinear with the stripes. The contrast for the direct observation of charge order arises from the different energy dependence of the $(2p \rightarrow 3d)$ excitation process for Ni ions with and without the extra holes introduced by doping. The strong resonance found here demonstrates the extreme sensitivity of resonant soft-x-ray diffraction.

While some information can be obtained from a qualitative analysis, e.g., from a comparison of the La and the Ni resonance, the full power of soft x-ray resonant diffraction evolves from a combination with a quantitative microscopic theory. The theory we present here is an extension of that by Castleton and Altarelli [16]; while they used an ionic model, we apply the more realistic configuration-interaction cluster model, which is widely accepted for the analysis of high-energy spectra from transition metal compounds [15]. This model properly treats the essential coupling between metal ions and the oxygen ligands,

which is the physical reason for, e.g., a Zhang-Rice-like [24,25] scenario.

The scattering intensity $I(\omega)$ as a function of the incoming photon energy ω can be described as

$$I(\omega) = \left| \sum_n e^{i\boldsymbol{q}\cdot\boldsymbol{R}_n} (\boldsymbol{\varepsilon}'^{*} \cdot F_n(\omega)\boldsymbol{\varepsilon}) \right|^2, \quad (1)$$

where $\boldsymbol{q}$ denotes the scattering vector, $\boldsymbol{R}_n$ is the position of the nth Ni ion site, $\boldsymbol{\varepsilon}$ ($\boldsymbol{\varepsilon}'$) is the incoming (outgoing) photon polarization vector, and the 3×3 tensor $F_n(\omega)$ describes the polarization-dependent scattering amplitude at the site n. Stripes with a periodic order Ni^{3+}, Ni^{2+}, Ni^{2+}, Ni^{3+}, Ni^{2+}, Ni^{2+}, Ni^{2+} are assumed in the model, with the Ni^{3+} stripes serving as antiphase domain walls for the antiferromagnetic order of the Ni^{2+} spins, which are canted by about 10° in the a-b plane with respect to the stripes. Such an arrangement produces spin- and charge-order diffraction peaks with $\epsilon = 2/7 \approx 0.286$, which is close to the experimental value.

We consider for each Ni^{2+} (Ni^{3+}) ion site a NiO_6^{10-} (NiO_6^{9-}) cluster with the D_{4h} symmetry, where the ten Ni $3d$ states and the nearest-neighbor oxygen $2p$ states are taken into account. The resonant scattering is treated as a second-order optical process, in which a Ni ion with a configuration $2p^6 3d^n$ is excited to the intermediate state with $2p^5 3d^{n+1}$ by the $2p \rightarrow 3d$ electric dipole transition:

$$F_n(\omega) = k^2 \langle n|\boldsymbol{P} \frac{1}{E_n + \hbar\omega - H_m + i\Gamma_m/2} {}^t\boldsymbol{P}|n\rangle, \quad (2)$$

where k denotes the wave number of the incoming photon, E_n and $|n\rangle$ are the ground state eigenvalue and eigenfunction, H_m and Γ_m are the Hamiltonian and lifetime width of the intermediate state, and $\boldsymbol{P} = -e\sum_i \boldsymbol{r}_i$ is the electric dipole operator. Coulomb and exchange interactions between $3d$ electrons, $3d$ spin-orbit interaction, and hybridization between the Ni $3d$ and the oxygen $2p$ orbitals are taken into account in the calculation of E_n and $|n\rangle$. Coulomb and exchange interactions between $3d$ electron and $2p$ core hole and $2p$ spin-orbit interaction are included in H_m. A small molecular field $H_{mol} = 0.02$ eV is applied for the Ni^{2+} sites to induce spin moments. The values for the model parameters are the standard ones often used for nickel-oxide materials [15,29], except that here the in-plane hybridization strength $(pd\sigma)_1$ is set at a value of -1.88 eV, which is higher than the out-of-plane $(pd\sigma)_2$ of -1.12 eV, to account for the much shorter in-plane Ni-O bond length. $\Gamma_m = 0.15$ eV (0.2 eV) at the L_3 (L_2) edge and a Gaussian broadening with a width of 0.2 eV (HWHM) are applied; the latter is close to the nominal beam line resolution of 0.15 eV.

With this single set of parameters, we are able to explain the shape of the spectra including the relative intensities of the different diffraction signals (Fig. 2). The model also reproduces the experimental Ni contribution to the x-ray absorption spectrum [Fig. 2(e)], which was determined by subtracting out the La contribution obtained from $LaTiO_3$. The agreement for the spin- and charge-order spectra is satisfactory. The energy positions of the peaks, shoulders, and valleys are in most cases well reproduced, including the 1 eV energy shift between the π and σ polarization for the charge-order L_3 resonance. There are deviations, e.g., at the L_2 resonance for the spin order (π) and charge order (σ), and we speculate that perhaps the influence of the La ions needs also to be included in a more extensive model.

The analysis provides a detailed understanding of the ground state in the charge-ordered phase: At the Ni^{3+} sites, where the effective charge-transfer energy $\Delta_{3+} = \Delta_{2+} - U_{dd}$ is negative, the doped holes reside mainly in the oxygen ligand molecular orbital with $x^2 - y^2$ symmetry. The $3d$ electron count at the Ni^{3+} sites is as high as 7.9, which is surprisingly not much smaller than the 8.2 for the Ni^{2+}. The spins of the holes on the ligand and $3d$ orbitals couple antiferromagnetically and form an $S = 1/2$ state [9,30] in which the Ni ion with $t_{2g}^6 e_{g\uparrow}^2$ configuration is dressed with a hole in the $(x^2 - y^2)\uparrow$ ligand orbital. This state is analogous to the Zhang-Rice singlet state in a cuprate superconductor [24,25]. This assignment is strongly supported by the observation that between the two polarizations there is a strong shift of about 1 eV in the peak maxima in each of the L_2 and L_3 edges of the $(2\epsilon, 0, 1)$ spectrum, which indicates a large energy splitting of the unoccupied $x^2 - y^2$ and $3z^2 - r^2$ levels. Since only the polarization vector of π-polarized light has a finite projection on the c axis, the

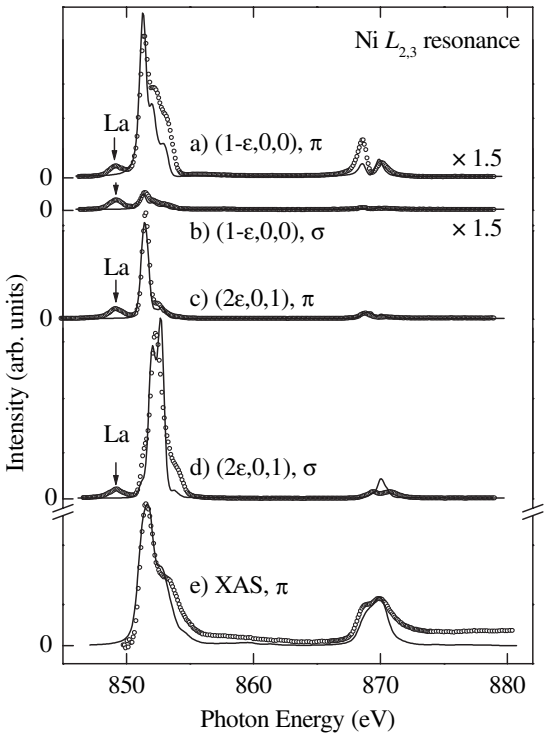

FIG. 2. Comparison between measured data (symbols) and the results of the cluster simulation. The simulated diffraction spectra have been scaled by one common factor to match the experiment. The La M_4 peaks at 849.2 eV, marked by arrows, are not included in the Ni $L_{2,3}$ simulation.

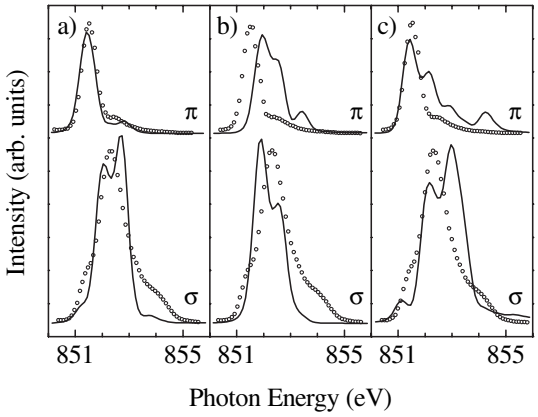

FIG. 3. Sensitivity of the simulated spectra to the model as seen at the L_3 resonance of the $(2\epsilon, 0, 1)$ charge-order peak: the oxygen holes are (a) confined in-plane and antiferromagnetically coupled to the Ni, (b) not confined in-plane $[(pd\sigma)_1 = (pd\sigma)_2 = -1.88$ eV], (c) ferromagnetically coupled to the Ni ($U_{dd} = 2$ eV). The circles are the experimental data.

transition probability of the $2p$-core electron to the low-lying $3z^2 - r^2$ orbital, having lobes along the c axis, is much higher with π than with σ polarization, for which the excitation into the $x^2 - y^2$ orbital dominates. With such a large level splitting, the doped holes can be considered to be well confined in-plane and the system possesses strong two-dimensionality-like cuprates.

In order to illustrate the reliability of our analysis we present in Fig. 3 also a scenario in which the oxygen hole is not confined in-plane [Fig. 3(b)] or is ferromagnetically coupled to the Ni [Fig. 3(c)]. One can clearly see significant deviations from the experimental data (Fig. 3, circles) and the antiferromagnetic or in-plane scenario. If the oxygen hole is not confined in-plane, the 1 eV energy shift in the polarization dependence is missing and the line shape of the π signal is too broad; if the oxygen hole is ferromagnetically coupled, there is by far too much intensity on the high-energy side of the peaks.

To conclude, we have observed well developed superstructures in $La_{1.8}Sr_{0.2}NiO_4$ using resonant soft x-ray diffraction. The intensities of the spin-order and charge-order diffraction peaks show strong enhancements when x-ray energies are tuned to the vicinity of the Ni $L_{2,3}$ absorption edges. These observations show directly that not only the antiferromagnetic but also the charge order resides within the NiO_2 layers. The photon-energy and polarization dependence of the charge and spin-order diffraction intensity across the Ni $L_{2,3}$ edges can be reproduced by a quantitative microscopic model calculation assuming stripes of Ni^{2+}- and Ni^{3+}-like ions, in which the Ni^{3+}-like objects are formed of a Ni^{2+} ion accompanied by a hole, which is essentially located at the surrounding in-plane oxygen ions in analogy to a Zhang-Rice singlet in cuprate systems.

We gratefully acknowledge the expert support and excellent working conditions at BESSY. We thank L. Hamdan and R. Bauer for their skillful technical assistance, T. Koethe for help in preparing the experiment, as well as A. Rusydi and P. Abbamonte for their help during preparational soft-x-ray diffraction experiments at the National Synchrotron Light Source at Brookhaven. The research in Köln is supported by the Deutsche Forschungsgemeinschaft through SFB 608, and the work in Berlin by the BMBF Project No. 05 KS1 KEE/8.

[1] C. H. Chen, S.-W. Cheong, and A. S. Cooper, Phys. Rev. Lett. **71**, 2461 (1993).
[2] J. M. Tranquada, D. J. Buttrey, V. Sachan, and J. E. Lorenzo, Phys. Rev. Lett. **73**, 1003 (1994).
[3] V. Sachan *et al.*, Phys. Rev. B **51**, 12 742 (1995).
[4] J. M. Tranquada *et al.*, Nature (London) **375**, 561 (1995).
[5] V. Hinkov *et al.*, Nature (London) **430**, 650 (2004).
[6] T. Hanaguri *et al.*, Nature (London) **430**, 1001 (2004).
[7] T. Hotta and E. Dagotto, Phys. Rev. Lett. **92**, 227201 (2004).
[8] P. Kuiper *et al.*, Phys. Rev. B **44**, 4570 (1991).
[9] E. Pellegrin *et al.*, Phys. Rev. B **53**, 10 667 (1996).
[10] A. Sahiner *et al.*, Phys. Rev. B **53**, 9745 (1996).
[11] P. Kuiper *et al.*, Phys. Rev. B **57**, 1552 (1998).
[12] J. Luo, G. T. Trammell, and J. P. Hannon, Phys. Rev. Lett. **71**, 287 (1993).
[13] F. M. F. de Groot, J. Electron Spectrosc. Relat. Phenom. **67**, 529 (1994).
[14] See review in the Theo Thole Memorial Issue, J. Electron Spectrosc. Relat. Phenom. **86**, 1 (1997).
[15] A. Tanaka and T. Jo, J. Phys. Soc. Jpn. **63**, 2788 (1994).
[16] C. W. M. Castleton and M. Altarelli, Phys. Rev. B **62**, 1033 (2000).
[17] C. Schüßler-Langeheine *et al.*, J. Electron Spectrosc. Relat. Phenom. **114–116**, 953 (2001).
[18] P. Abbamonte *et al.*, Science **297**, 581 (2002).
[19] S. B. Wilkins *et al.*, Phys. Rev. Lett. **91**, 167205 (2003).
[20] S. S. Dhesi *et al.*, Phys. Rev. Lett. **92**, 056403 (2004).
[21] K. J. Thomas *et al.*, Phys. Rev. Lett. **92**, 237204 (2004).
[22] P. Abbamonte *et al.*, Nature (London) **431**, 1078 (2004).
[23] E. Weschke *et al.*, Phys. Rev. Lett. **93**, 157204 (2004).
[24] F. C. Zhang and T. M. Rice, Phys. Rev. B **37**, R3759 (1988).
[25] H. Eskes and G. A. Sawatzky, Phys. Rev. Lett. **61**, 1415 (1988).
[26] E. Weschke *et al.* (to be published).
[27] The change of the probing volume caused by the variation of the photon mean-free path and incidence and detection angle across the resonance has been corrected for using the absorption coefficient μ as obtained from the x-ray absorption spectrum [28].
[28] J. Als-Nielsen and D. McMorrow, *Elements of Modern X-ray Physics* (Wiley, New York, 2001).
[29] $U_{dd} = 7.0$ eV, $U_{\mathrm{dc}} = 8.5$ eV, $\Delta_{2+} = 6.5$ eV (for Ni^{2+}), $10Dq = 0.5$ eV, $(pd\pi) = -\sqrt{3}/4(pd\sigma)$ [15].
[30] P. Kuiper *et al.*, Phys. Rev. Lett. **62**, 221 (1989).